Science of the Total Environment 624 (2018) 758–768

Contents lists available at ScienceDirect

Science of the Total Environment

journal homepage: www.elsevier.com/locate/scitotenv

Dissolution and transport of insensitive munitions formulations IMX-101 and IMX-104 in saturated soil columns

Jennifer D. Arthur [a], Noah W. Mark [a], Susan Taylor [b], Jiří Šimůnek [c], Mark L. Brusseau [a,d], Katerina M. Dontsova [a,e,*]

[a] Soil, Water and Environmental Science Department, University of Arizona, United States
[b] U.S. Army Engineer Research and Development Center, United States
[c] Department of Environmental Sciences, University of California, Riverside, United States
[d] Department of Hydrology & Atmospheric Sciences, University of Arizona, United States
[e] Biosphere 2, University of Arizona, United States

HIGHLIGHTS

- Dissolution and transport experiments were performed for IMX-101 and IMX-104
- IM constituents dissolved in order of their solubility
- NTO and NQ concentrations were high initially but decreased with time
- Modified HYDRUS-1D successfully described both dissolution and transport of IMs
- Determined transport parameters agreed with values obtained in batch studies

GRAPHICAL ABSTRACT

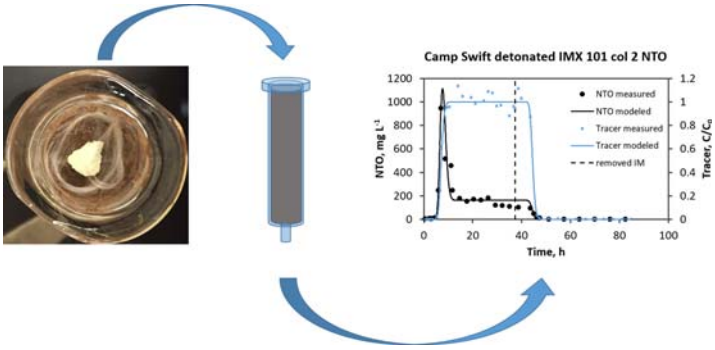

ARTICLE INFO

Article history:
Received 5 October 2017
Received in revised form 11 November 2017
Accepted 27 November 2017
Available online xxxx

Editor: Dr. Ouyang Wei

Keywords:
Insensitive munitions
Dissolution
HYDRUS-1D modeling
IMX formulations
2, 4-Dinitroanisole (DNAN)
3-Nitro-1,2,4-triazol-5-one (NTO)

ABSTRACT

Military training exercises can result in deposition of energetic residues on range soils, which ultimately can contaminate groundwater with munitions constituents. Column experiments followed by HYDRUS-1D modeling were conducted to evaluate dissolution and transport of energetic constituents from the new insensitive munitions (IM) formulations IMX-101, a mixture of 3-nitro-1,2,4-triazol-5-one (NTO), nitroguanidine (NQ), and 2, 4-dinitroanisole (DNAN), and IMX-104, a mixture of NTO, 1,3,5-hexahydro-1,3,5-trinitro-1,3,5-triazine (RDX) and DNAN. NTO and DNAN are emerging contaminants associated with the development of insensitive munitions as replacements for traditional munitions. Flow interruption experiments were performed to investigate dissolution kinetics and sorption non-equilibrium between soil and solution phases. The results indicated that insensitive munitions compounds dissolved in order of their aqueous solubility, consistent with prior dissolution studies conducted in the absence of soil. Initial elution of the high concentration pulse of highly soluble NTO and NQ was followed by lower concentrations, while DNAN had generally lower and more constant concentrations in leachate. The sorption of NTO and NQ was low, while RDX, 1,3,5,7-octahydro-1,3,5,7-tetranitrotetrazocine (HMX, an impurity in technical grade RDX), and DNAN all exhibited appreciable sorption. DNAN transformation was observed, with formation of amino-reduction products 2-ANAN (2-amino-4-nitroanisole) and 4-ANAN (4-amino-2-nitroanisole). HYDRUS-1D model, incorporating one-dimensional advective-dispersive transport with particle dissolution and first-order solute transformation was used to simulate the measured breakthrough curves. Optimized dissolution parameters varied widely but were correlated between compounds in the same formulation. Determined

* Corresponding author at: Biosphere 2, University of Arizona, 845 N. Park Avenue, Tucson, AZ 85721-0158, United States.
E-mail address: dontsova@email.arizona.edu (K.M. Dontsova).

https://doi.org/10.1016/j.scitotenv.2017.11.307
0048-9697/

adsorption coefficients generally agreed with values determined from batch and column studies conducted with pure NTO and DNAN, while mass-loss rate coefficients were in better agreement with ones from batch than column studies possibly due to suppression of microbial transformation during elution of high concentrations of explosives. Even in the low organic matter soils selected in this study DNAN experienced significant retardation and transformation, indicating potential for its natural attenuation.

1. Introduction

The United States Army and BAE systems (Arlington, VA) have developed insensitive munitions (IM) formulations to replace 2,4,6-trinitrotoluene (TNT) and Composition B, which contains 1,3,5-trinitro-1,3,5-triazine (RDX) and TNT, because TNT and RDX can be vulnerable to temperature and shock causing unintended detonations. Two explosive compounds, 3-nitro-1,2,4-triazol-5-one (NTO) and 2, 4-dinitroanisole (DNAN) have been selected as replacements. The IM formulations that have been developed using NTO and DNAN are IMX-101 (19.7% NTO, 36.8% nitroguanidine (NQ), and 43.5% DNAN) and IMX-104 (53.0% NTO, 15.3% RDX, and 31.7% DNAN). DNAN serves as a binder in these melt-cast explosive formulations. IMX-104 also has 1,3,5,7-octahydro-1,3,5,7-tetranitrotetrazocine (HMX) present because technical grade RDX contains approximately 10% HMX.

When munitions do not completely detonate (a low-order detonation), a significant mass of the explosive compounds originally present in a round can be deposited on the ground. Training ranges are a particular concern due to the great number of rounds fired in the same location, resulting in some cases in groundwater contamination with munitions constituents (Jenkins et al., 2001). The likelihood of IM rounds experiencing low-order detonations is higher than for rounds filled with traditional explosives (Walsh et al., 2013). Hence, more IM explosives will likely be deposited on the ground compared to traditional explosives. When explosives are exposed to rainfall, they dissolve, introducing the munitions constituents into the environment. Transport of explosive compounds off military ranges can result in closure of the ranges or limit training.

Health and environmental effects associated with exposure to explosive compounds vary. Toxicological reports for NTO indicate that is it not toxic to rats and mice when given orally ($LD_{50} > 5\ g \cdot kg^{-1}$) (London and Smith, 1985). Nitroguanidine has low toxicity in mammals, as well: the reported oral LD_{50} for NQ is 3.9 $g \cdot kg^{-1}$ in mice and 10.2 $g \cdot kg^{-1}$ in rats (Deeter, 2000). NQ also has low acute and chronic toxicity to a range of aquatic organisms; however, products of NQ photolysis have been shown to be 100-fold more toxic (Burton et al., 1993; Sunahara, 2009). RDX and DNAN have higher mammalian and ecotoxicity: RDX's reported LD_{50} ranges from 44 to 300 $mg \cdot kg^{-1}$ in rats and the major toxic effects include anemia with secondary splenic lesions, hepatotoxicity, possible effects on the central nervous system, and urogenital lesions (Etnier, 1986; Deeter, 2000). Toxicological reports for DNAN indicate that it is more toxic than TNT for mammals (LD50 (rat) of 199 $mg \cdot kg^{-1}$) (Davies and Provatas, 2006) and is toxic to bacteria *Vibrio fischeri* and freshwater green algae *Pseudokirchneriella subcapitata* in the $mg \cdot L^{-1}$ range and to earthworm *Eisenia andrei* and perennial ryegrass *Lolium perenne* in the $mg \cdot kg^{-1}$ range (Dodard et al., 2013).

The high aqueous solubilities of NTO and NQ indicate that both compounds will more readily dissolve in water than DNAN and RDX, which are substantially less soluble (Table 1). Laboratory drip tests show that the aqueous solubility of the IMX formulations controls their dissolution, with NTO dissolving 1st followed by NQ, and DNAN in IMX-101 and by RDX and DNAN in IMX-104 (Taylor et al., 2013; Taylor et al., 2015b). Concentrations of NTO and NQ in aqueous solutions were high initially when the compounds were dissolving from the outer shell of IM particles, but decreased with time as the distance between particle surface and dissolving compounds increased. Dissolution of NTO and NQ from IMX-101 and NTO from IMX-104 left a porous particle comprised of DNAN (and RDX for 104) whose dissolution was more constant over time (Taylor et al., 2013). This dissolution pattern was also observed in outdoor dissolution studies, where in addition photo-transformation of IM compounds was observed (Taylor et al., 2015a).

Parameters that describe interaction of munitions constituents with soils, linear (K_d) and Freundlich (K_f) soil adsorption coefficients, soil organic carbon (OC) adsorption coefficients (K_{OC}), as well as octanol–water partition coefficients, K_{ow}, have been reported for the traditional components of these formulations, NQ and RDX, and to a lesser extent for NTO and DNAN (Table 1). NQ and NTO are both very mobile and have low $K_{d,}$ K_{OC}, and K_{ow} values (Mirecki et al., 2006; Mark et al., 2016; Mark et al., 2017) (Table 1). Mark et al. (2016) examined NTO interactions with a number of soils and concluded that adsorption was low and not related to the amount of OC in the soil, but was strongly influenced by soil pH due to the ionic character of NTO. Mark et al. (2016, 2017) also indicated that NTO transformation rates are sensitive to soil OC content. In agreement with its low K_{ow} values (Burrows et al., 1989; Dave et al., 2000), NQ experiences little adsorption in soils (Dontsova et al., 2007; Dontsova et al., 2008; Taylor et al., 2012). It also does not transform, resulting in conservative transport through soils (Dontsova et al., 2007; Dontsova et al., 2008; Taylor et al., 2012).

DNAN has a higher K_{ow} value than NQ, NTO and RDX, and thus is anticipated to be less mobile in soil (Table 1). Batch and column soil adsorption experiments for DNAN (Arthur et al., 2017) indicated that DNAN strongly adsorbed to soils, resulting in significant retardation during transport. Linear adsorption coefficients measured in batch studies for 11 different soils ranged between 0.6 and 6.3 $L \cdot kg^{-1}$, and Freundlich coefficients between 1.3 and 34 $mg^{1-n} \cdot L^{n} \cdot kg^{-1}$ and positively correlated with cation exchange capacity and the amount of OC in the soil. It was also shown that DNAN is readily reduced to amino transformation products 2-amino-4-nitroanisole (2-ANAN) and 4-amino-2-nitroanisole (4-ANAN) (Hawari et al., 2015; Arthur et al., 2017). RDX has intermediate behavior with higher K_d, K_{OC}, and K_{ow} values than NTO and NQ, but lower than for DNAN (Haderlein et al., 1996; Singh et al., 1998). The results of a study examining NTO and DNAN sorption from IMX-101 solutions (Richard and Weidhaas, 2014) showed that the Freundlich isotherm provided the best fit of both data sets, and that desorption was limited.

The objective of this study was to examine the dissolution and fate (adsorption and transformation) of IMX-101 and IMX-104 in two soils collected from military training ranges in Camp Swift, TX and Camp Guernsey, WY. The results are assessed and compared to the dissolution studies without soils and transport and fate behavior observed for individual constituents of the insensitive munitions formulations.

2. Materials and methods

2.1. Soils

Camp Swift (Bergstrom sandy clay loam, mixed, superactive, thermic Cumulic Haplustolls) collected at Camp Swift, TX and Camp Guernsey (Keeline-Turnercrest loam, mixed, superactive, calcareous, mesic Ustic Torriorthents) collected in Camp Guernsey, WY were the soils used for this study. These two soils were previously used in batch and column transport experiments conducted with NTO and DNAN (Dontsova et

Table 1
Environmentally relevant chemical and physical properties of DNAN, NTO, NQ, RDX, and HMX including solubility at 25 °C, octanol-water partition coefficient (K_{ow}), soil organic carbon adsorption coefficient (K_{OC}), and soil adsorption coefficient (K_d).

Property	DNAN	NTO	NQ	RDX	HMX
Solubility, mg·L^{-1}	276.2[a1]	16642[c2]	2600–5000[b3]	59.9[a4]	5[5]
Log K_{ow}	1.7–1.92[b], 1.62[a6], 1.58[a7]	0.37–1.03[b6]	−0.83[b8]	0.81–0.87[b4]	0.19[a9]
Log K_{OC}	2.2[b10], 2.33–2.56[a7], 1.93–2.63[a11]	2.1[b10], 0.60–1.79[a12]	−0.356[b13], 0.82–2.22[a14]	0.88–2.4[b4]	0.54–2.8[a15]
K_d, L·kg^{-1}	0.6–6.3[a11]	0.02–0.51[a12]	0.15–0.43[a16], 0.24–0.60[a17]	0.12–36[a14]	0.12–12.1[a14]

[a]Measured; [b]Estimated; [c]Interpolated from measured values. [1](Boddu et al., 2008); [2](Spear et al., 1989); [3](Mirecki et al., 2006); [4](Brannon and Pennington, 2002); [5](Glover and Hoffsommer, 1973); [6](Sokkalingam et al., 2008); [7](Hawari et al., 2015); [8](Dave et al., 2000); [9](Yoon et al., 2002); [10](Chakka et al., 2008); [11](Arthur et al., 2017); [12](Mark et al., 2016); [13](Burrows et al., 1989); [14](Dontsova and Taylor, 2018); [15](Boyer et al., 2007); [16](Pennington et al., 2004); [17](Taylor et al., 2012).

al., 2014; Mark et al., 2016; Arthur et al., 2017; Mark et al., 2017). These soils were selected for their relatively low organic matter content to provide conservative estimates of soil attenuation of IM compounds. Soil samples were collected to a depth of 30 cm; they were air-dried and sieved (<2 mm) prior to being analyzed for pH in 1:1 soil:water, electrical conductivity (EC), cation exchange capacity (CEC), OC content, and clay mineralogy (Mark et al., 2016). Both soils have high pH (7.83 and 8.21) and low OC content (0.34 and 0.77% for Camp Swift and Camp Guernsey, respectively), but differ in their particle size distribution. Camp Swift is finer textured (23.7% clay, 20.8% silt, and 55.5% sand) while Camp Guernsey is coarser (4.1% clay, 12.5% silt, and 83.4% sand). Cation exchange capacity is higher in Camp Swift: 6.5 cmol·kg^{-1} compared to 2.9 cmol·kg^{-1} in Camp Guernsey due to higher clay content; and both soils have mixed mineralogy with Camp Guernsey having more smectite (Mark et al., 2016).

2.2. Column experiments

To measure dissolution and transport behavior of IMX-101 and IMX-104, saturated flux-controlled column experiments were conducted under steady-state and transient conditions. Supelco (Belfonte, PA) glass columns with internal diameter of 1.18 cm and 7-cm length were used in this study. Columns were packed with Camp Guernsey and Camp Swift soils. The columns were packed in small increments to ensure uniform bulk density and to minimize preferential flow. Glass wool was placed on the top and bottom of the soil profile to prevent soil movement. The average packed bulk density (ρ_b) was 1.61 ± 0.05 g cm^{-3} for Camp Guernsey soil and 1.51 ± 0.04 g cm^{-3} for Camp Swift soil. The bulk density was determined from the dry mass of the soil used to pack the glass columns of known volume.

Columns were saturated from bottom to top with 0.005 M $CaCl_2$ background solution for one hour to avoid air entrapment. Pore volume (PV) of the columns was determined by measuring the volume of solution necessary to saturate the packed column, corrected for column dead volume. After this, approximately 50 mg of undetonated or detonated IMX-101 and IMX-104 was placed on top of the column on a layer of glass wool (Figure S1). Technical grade IMX-101 and IMX-104 used in the experiments (undetonated samples) were provided by the US Army Armament Research, Development and Engineering Center (ARDEC), Picatinny Arsenal, while detonated samples were residues of low order detonations (Walsh et al., 2014).

PTFE caps were used to seal the tops of the columns. Tygon microbore tubing connected PTFE caps with the Cole-Parmer (Vernon Hills, IL) Master flex peristaltic pump that supplied solution. Columns were connected to the pump on the top and flow of 0.005 M $CaBr_2$ tracer solution was started. Measured average flow rate was 0.008 ± 0.001 mL·min^{-1}, equivalent to Darcy flux of 0.42 ± 0.05 cm·h^{-1} and mean pore-water velocity of 1.06 ± 0.17 cm·h^{-1}. After three to five PV) for IMX-101 (five to eight PVs for IMX-104) depending on the soil, IM particles were removed and flow was switched to background solution (0.005 M $CaCl_2$) that was applied for another three to five PVs to monitor the elution of the munitions constituents from the soil. In addition, flow interruption studies were conducted, where flow was stopped for 24 h to better characterize potential mass-transfer processes. This technique is used to differentiate between different mechanisms responsible for sorption non-equilibrium (Brusseau et al., 1989; Brusseau et al., 1997) and study dissolution kinetics (Dontsova et al., 2008; Dontsova et al., 2009; Taylor et al., 2012).

Effluent samples were collected continuously into 4-mL amber vials using a Teledyne ISCO (Lincoln, NE) Foxy 200 Fraction collector with a 200-vial capacity. A conservative tracer, Br^-, was used to determine the longitudinal dispersivity (λ) and observe for preferential flow for each soil. Br^- was analyzed using Ion Chromatography (Dionex ICS 5000 with diode array). High performance liquid chromatography was used to quantify eluting IM components as described below. Upon completion of each experiment, columns were subdivided into thirds (top, middle, bottom) and soil extractions were performed using acetonitrile (1:2 soil to acetonitrile). The suspensions were agitated for 24 h, centrifuged and filtered using 0.45 μm Millex-HV PVDF filter (EMD Millipore Darmstadt, Germany) (U. S. Environmental Protection Agency, 1994), and subjected to HPLC analysis.

Mass balance calculations were performed for all IM components by integration of each breakthrough curve (BTC), performing soil extractions, and extractions of remaining IM particles. Initial amount of IM compound in each particle was estimated assuming ideal mixing of the components.

Eight continuous flow dissolution and transport experiments (2 soils * detonated / undetonated * 2 replications) and four interrupted flow experiments (2 soils * detonated only * 2 replications) were conducted for each IM formulation. A total of twenty-four experiments were conducted, with a fresh pack used for each one.

2.3. Analytical method

Column effluent was analyzed for energetic compounds and their transformation products using a high performance liquid chromatograph (HPLC, Dionex Ultimate 3000) equipped with a diode array detector (ThermoFisher, MA). The method for NTO was adapted from Le Campion et al. (1999). The parameters used for analyzing NTO samples were the following: mobile phase ratio of acetonitrile (ACN): deionized water of 75:25 with 0.1% trifluoroacetic acid (TFA) was run isocractically at 1 mL·min^{-1}. Oven temperature was set at 32 °C. NTO and its transformation products were separated using a Thermo Scientific Hypercarb Column. NTO was detected at approximately 2.8 min using 315 nm wavelength. The UV detector was set at 220 nm to monitor for presence of potential NTO transformation product, 5-amino-1,2,4-triazol-3-one (ATO) (Le Campion et al., 1999). No ATO was detected. The operational method for DNAN, RDX, NQ, HMX and DNAN transformation products was adapted from Olivares et al. (2013). The following parameters were used to analyze these samples: a mobile phase ratio of 43:57 methanol and water; the Thermo Scientific Acclaim reversed phase column C-18 with 5-μm particle size; and a flow rate of 1 mL·min^{-1}. The wavelengths used for detection and quantification were 300 nm for DNAN, NQ, 254 nm for 2-ANAN, 4-ANAN, RDX, HMX, and 210 nm for DAAN. The retention times for each compound on HPLC were for DNAN approximately 21 min, 11 min for 2-ANAN, 6 min for 4-ANAN, 8 min for RDX, 5 min for HMX, and 3 min for NQ. Detection limits were 0.015 mg·L^{-1} for DNAN, 2-ANAN, 4-ANAN, NQ, RDX, HMX, and 0.020 mg·L^{-1} for

NTO as determined by visual evaluation of the standard curve for each compound.

2.4. Numerical analysis

All experiments were analyzed using the HYDRUS-1D code for simulating the one-dimensional movement of water, heat and multiple solutes in variably saturated porous media (Šimůnek et al., 2008; Šimůnek and van Genuchten, 2008). HYDRUS-1D is a numerical model that solves the governing flow and transport equations using the method of finite elements. The software was used in the inverse mode to analyze BTCs obtained in the column experiments. HYDRUS-1D was modified to account for dissolution of constituents from solids. Similar modifications have been used in previous studies (Dontsova et al., 2006; Dontsova et al., 2008; Dontsova et al., 2009; Taylor et al., 2012) to estimate the dissolution rates of energetic materials, explosives and propellants.

2.4.1. Dissolution

For explosive materials in this study, the DNAN, NTO, NQ, HMX, and RDX dissolution rate, Υ, was defined as:

$$\Upsilon = max\left(\Upsilon_{max} e^{-\chi t}, \Upsilon_{min}\right) \quad (1)$$

where Υ_{max} is the initial (maximum) dissolution rate [$ML^{-3}\cdot T^{-1}$], χ is the decay constant [T^{-1}], Υ_{min} is the minimum or steady-state dissolution rate, defined as a product of Υ_{max} and a, the dimensionless constant, and t is time [T]. If $\Upsilon_{max} e^{-\chi t} > \Upsilon_{min}$ then $\Upsilon_{max} e^{-\chi t}$ is used in the equation. If $\Upsilon_{max} e^{-\chi t} < \Upsilon_{min}$ then Υ_{min} is used. Dissolution rates are reported normalized to the mass of the IMX-101 or 104 added to the column (Taylor et al., 2012).

2.4.2. Reactive transport

The transport equation for constant flux density, water content, dispersion coefficient, bulk density, and distribution coefficient is

$$\frac{\partial \Theta C}{\partial t} = D^* \left(\frac{\partial^2 C}{\partial z^2}\right) - \frac{\partial qC}{\partial z} - \frac{\rho_b \partial S}{\Theta \partial t} - \varphi + \Upsilon\Theta \quad (2)$$

where Θ represents the volumetric water content [$L^3\cdot L^{-3}$], C is the concentration of the solution [ML^{-3}], z represents the spatial coordinate [L], q is the volumetric fluid flux density [LT^{-1}] evaluated by Darcy–Buckingham law, ρ_b is the bulk density [ML^{-3}], Υ is the dissolution rate as described in Eq.1 [$ML^{-3}\cdot T^{-1}$], and D is the dispersion coefficient which accounts for both hydrodynamic dispersion and diffusion [$L^2\cdot T^{-1}$] which is represented in Eq. 3.

$$D = \lambda v + D^* \quad (3)$$

where v is the average linear velocity [LT^{-1}], λ is the longitudinal dispersivity [L], and D^* represents the effective diffusion coefficient [$L^2\cdot T^{-1}$]. Sorption, S, [MM^{-1}] is assumed to be instantaneous and is defined as:

$$S = K_d C \quad (4)$$

where K_d is the linear adsorption coefficient [$L^3\cdot M^{-1}$]. φ is the sink/source term which accounts for zero-, first- and other-order reactions [$ML^{-3}\cdot T^{-1}$]. In this model, φ is the first-order rate for the solution only [$ML^{-3}\cdot T^{-1}$] and is defined for IM constituents as:

$$\varphi = k\,\Theta\,C \quad (5)$$

where k represents the mass-loss rate coefficient due to transformation and/or irreversible adsorption [T^{-1}]. Lastly, for the daughter products, the first-order reaction rate [$ML^{-3}\cdot T^{-1}$] is defined as:

$$\varphi = k\,\theta C_w - k_p\,\theta\,C_{wp} \quad (6)$$

where the first term on the right side represents transformation of a daughter product (i.e., 2-ANAN) and the second term represents production of a daughter product by transformation of a parent compound (i.e., DNAN). In eq. 6, k_p and C_{wp} represent the transformation rate constant [T^{-1}] and solute concentration [ML^{-3}] of a parent compound. Bromide tracer values for k and K_d were equal to zero.

2.4.3. Parameter estimation

Numerical analysis of the experimental data was performed by first using the nonreactive tracer data to determine λ (cm). The dispersivity for explosives was fixed at the values determined for the tracer. The following parameters were optimized for the munitions constituents: K_d ($L\cdot kg^{-1}$) and dissolution parameters, Υ_{max}, χ, and constant, a, which multiplied by Υ_{max} gives the steady-state dissolution rate (Υ_{min}) ($mg\cdot L^{-1}\cdot h^{-1}$). The mass-loss rate coefficient for dissolved phase, k (h^{-1}) (transformation rate constant) was set to values determined from batch studies for DNAN and NTO (Mark et al., 2016; Arthur et al., 2017) and derived from literature for NQ, RDX, and HMX. Conversely, they were optimized via HYDRUS-1D for 2-ANAN. The 95% confidence intervals and R^2 values for optimized parameters were obtained by statistical analysis of the predicted versus measured breakthrough curves. Parameter estimates were considered significant if they were statistically different than zero. For the replicate experiments parameter estimates were averaged and differences determined based on confidence intervals of the mean.

3. Results and discussion

3.1. Tracer

Measured bromide BTC are symmetrical, occur at one PV, and are well described using the advection-dispersion transport model (Figs. 1, 2, 4, and 5). This indicates ideal advective-dispersive transport, with no measurable impacts of preferential flow or air entrapment within the column (e.g., Brusseau, 1994). Longitudinal dispersivity was slightly larger for the coarser Camp Guernsey soil (0.57 ± 0.32 cm) (mean ± CI) than for Camp Swift (0.20 ± 0.13 cm) but differences were not significant. The dispersivity values are consistent with values measured in prior column experiments (e.g., Brusseau, 1994).

3.2. IMX-101

All IMX-101 components, NTO, NQ, and DNAN, as well as 2-ANAN and 4-ANAN, transformation products of DNAN, were observed in the effluent from both detonated and undetonated IMX-101 (Fig. 1). The IM constituents BTCs followed a general pattern of high initial peak in effluent concentration, followed by a rapid decrease to a relatively steady-state stage. This pattern was very pronounced for NTO and NQ, while for DNAN effluent concentrations were relatively constant once breakthrough occurred. NTO had the highest maximum outflow concentrations in all experiments despite representing only 19.7% of the total mass of IMX-101. The high concentrations of NTO seen in the effluent are consistent with its high solubility and rapid dissolution observed in laboratory drip studies (Taylor et al., 2013; Taylor et al., 2015b). Initial peak concentrations of NQ, on the other hand, were lower than those of NTO, despite higher content in the formulation (36.8%) but consistent with NQ solubility being lower by a factor of four (Table 1).

The suggested mechanism explaining the shape of the BTCs is that the initial higher concentrations are produced by ready dissolution of the IM constituents adjacent to the external surfaces of the IM particles, faster for more soluble components, and slower for less soluble ones. Whereas the reduction in concentrations that follows is related to slower release of constituents deeper within the matrix, where it is limited by time needed for water to reach particle interior and for solutes to exit the particle through convection and diffusion. Observed dissolution patterns are similar to ones described for propellant constituents that have

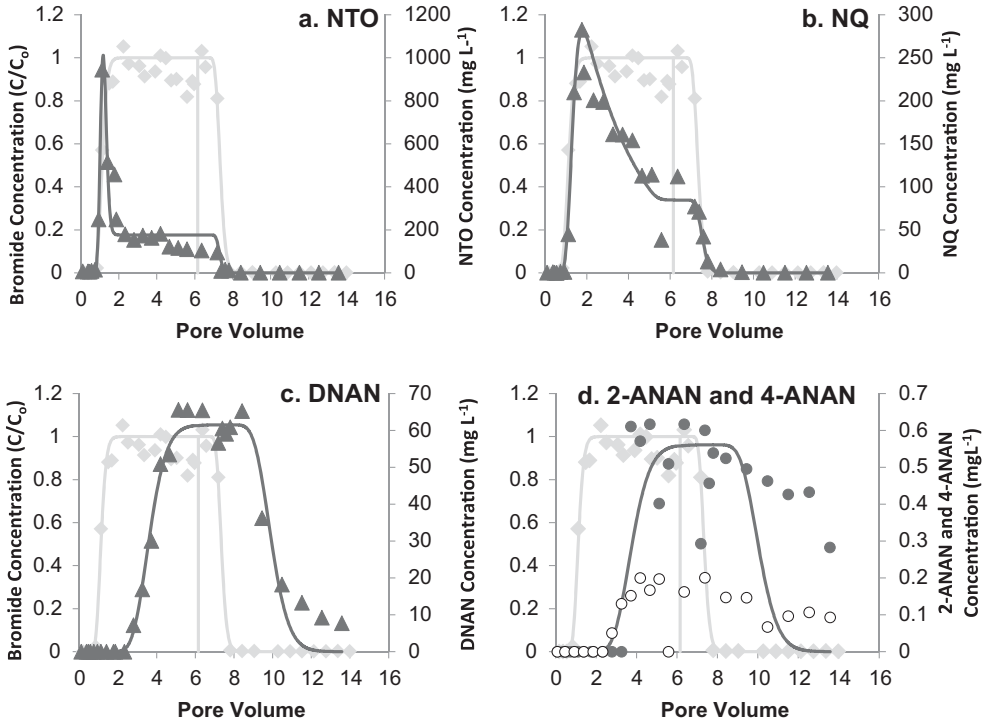

Fig. 1. Breakthrough curves for IM constituents dissolving from detonated IMX-101 in Camp Swift soil. Measured Br^- concentrations are presented in light grey diamonds, IM constituents, NTO, NQ, DNAN in dark grey triangles; and products of DNAN transformation, 2-ANAN and 4-ANAN, in solid and hollow circles, respectively. Lines present HYDRUS-1D simulation results. Vertical grey solid line indicates switch to background solution.

an insoluble nitrocellulose matrix (Dontsova et al., 2008; Dontsova et al., 2009; Taylor et al., 2011; Taylor et al., 2012), but are unlike what was observed for traditional explosive formulations that have overall less soluble constituents than IMs (Dontsova et al., 2006; Taylor et al., 2009).

While constituent concentrations in solution and estimated dissolution parameters differed between individual columns (Tables 2 and s1), HYDRUS-1D simulated Υ_{max} parameters had a highly significant correlation between NTO and DNAN (Fig. 2, $P = 0.000423$), indicating a link between dissolution of constituents from the IM particles. There was no significant difference between Υ_{max}, Υ_{min}, and χ parameter estimates for all IMX-101 constituents between experiments with undetonated and detonated IMs (Table 2 and s1). Parameter estimates for IMX-101 from lab drip studies (Taylor et al., 2015b) (Table s2) underestimated the dissolution parameters in this study, possibly due to larger size, and therefore lower specific surface area, of the particles they used (Table s1).

NTO breakthrough occurred at the same time as nonreactive tracer Br^- for all IMX-101 experiments, detonated and undetonated, with and without flow interruption (Figs. 1 and 2). This indicates NTO experienced no measurable sorption by either soil. In solution NTO is present in its deprotonated form and is negatively charged at environmentally relevant pHs (Smith and Cliff, 1999), limiting its adsorption to largely negatively charged soil surfaces. Previous research conducted on soil

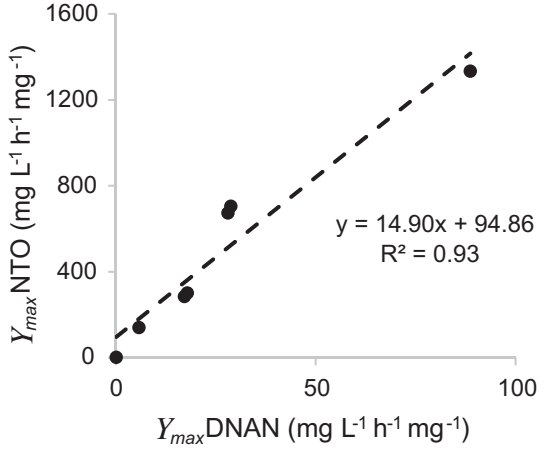

Fig. 2. Correlation between simulated initial dissolution rates, Υ_{max}, for NTO and DNAN, components in IMX-101 formulation from continuous flow experiments. The Thompson Tau method was used to reject 1 outlier in the data set.

Table 2
Mean dissolution parameters obtained by HYDRUS-1D for saturated column experiments involving IMX-101 in Camp Swift and Camp Guernsey soils. Decay constant, χ, and initial and steady-state dissolution rates, Υ_{max} and Υ_{min}, were estimated from explosives BTCs. FI = flow interruption and n = number of experiments included in the mean.

Treatment	χ	95% CI	Υ_{max}	95% CI	Υ_{min}	95% CI
			$mg \cdot L^{-1} \cdot h^{-1} \cdot mg^{-1}$		$mg \cdot L^{-1} \cdot h^{-1} \cdot mg^{-1}$	
NTO						
Detonated ($n = 4$)	0.66	0.36	349.99	223.13	10.30	11.12
Undetonated (n = 4)	1.04	1.13	585.25	564.20	11.40	8.11
Detonated FI (n = 4)	0.34	1.12	926.70	306.40	3.13	0.87
Mean across IMX-101 ($n = 12$)	0.68	0.40	620.65	248.15	8.28	4.69
NQ						
Detonated (n = 4)	0.76	0.82	177.11	136.16	19.15	20.63
Undetonated (n = 4)	1.91	3.07	143.86	120.40	8.65	5.96
Detonated FI (n = 4)	0.20	0.18	541.44	476.74	21.85	16.35
Mean across IMX-101 (n = 12)	0.96	1.05	287.47	187.06	16.55	8.81
DNAN						
Detonated (n = 4)	2.84	5.38	17.19	8.92	4.71	1.97
Undetonated (n = 4)	35.96	62.63	57.04	48.92	3.26	3.83
Detonated FI (n = 4)	4.00	7.35	35.18	16.21	13.97	10.07
Mean across IMX-101 (n = 12)	14.27	21.13	36.47	18.48	7.31	4.33

adsorption of NTO showed high mobility and low sorption (Braida et al., 2012; Hawari et al., 2012; Richard and Weidhaas, 2014; Mark et al., 2016; Mark et al., 2017). NTO K_d's were not significantly different from zero in HYDRUS-1D simulations for IMX-101 and therefore were set to zero for final optimization simulations (Table s1).

Similarly to NTO, NQ arrived with the nonreactive tracer indicating low soil adsorption (Figs. 1 and 2). Nitroguanidine is a relatively inert compound in soil environments: previous research has indicated limited adsorption of NQ in soils and little degradation/transformation (Haag et al., 1990b; Dontsova et al., 2007; Dontsova et al., 2008; Taylor et al., 2012). Estimated K_d's (Table s1) (0.06 ± 0.03 L·kg^{-1} for Camp Swift and 0.06 ± 0.04 L·kg^{-1} for Camp Guernsey) were on the lower range of literature values (Table 1) (Haag et al., 1990a; Pennington et al., 2004; Taylor et al., 2012) consistent with low OC content of the studied soils.

DNAN was the last compound to break through (Fig. 1). DNAN also had the lowest effluent concentrations. Previous research has shown that DNAN adsorbs to soil and that its adsorption is influenced by the soil OC and clay content (Hawari et al., 2015; Arthur et al., 2017). Linear adsorption coefficient values estimated by HYDRUS-1D for DNAN (Table s1) were similar for the two soils (0.63 ± 0.21 L·kg^{-1} for Camp Swift and 0.53 ± 0.07 L·kg^{-1} for Camp Guernsey). For Camp Swift soil, they were closer to batch experiment K_d's (0.60 ± 0.20 L·kg^{-1}) then those obtained from column experiment K_d values (1.2 ± 0.08 L·kg^{-1}) (Arthur et al., 2017).

2-ANAN and 4-ANAN, DNAN transformation products detected in column effluent also exhibited retardation (Figs. 1 and 2). They both appeared at the same time as DNAN for detonated and undetonated IMX-101. 2-ANAN concentrations in the effluent were approximately an order of magnitude lower than DNAN concentrations and 4-ANAN concentrations were smaller than 2-ANAN concentrations, indicating regio-selectivity of DNAN amino-transformation (Hawari et al., 2015; Arthur et al., 2017). Tailing occurred at the end of the experiments for 2-ANAN and 4-ANAN. Soil adsorption coefficients estimated for 2-ANAN (0.71 ± 0.52 L·kg^{-1} for Camp Swift and 1.56 ± 1.16 L·kg^{-1} for Camp Guernsey) (Table s1) were similar to the values determined in a column transport study of pure DNAN (0.43–1.93 L·kg^{-1}) and estimated k values for 2-ANAN (0.01 ± 0.01 h^{-1} for Camp Swift and 0.06 ± 0.03 h^{-1} for Camp Guernsey) were close to the estimated ks determined for 2-ANAN in Camp Swift soil in column transport studies (0.03 ± 0.04 h^{-1}) (Arthur et al., 2017). There were no significant differences between undetonated and detonated IMX-101 K_d values for all constituents (Table s1).

Flow interruption experiments were conducted for detonated IMX-101 only. After stopping flow and then resuming it in 24 h and elution of 1 PV, effluent NTO and NQ concentrations increased for both soils and then returned to steady-state values (Fig. 3). Increase in concentration after flow interruption is consistent with continuing dissolution of IM particles when flow is stopped causing solute accumulation. Once this solute passes through the column concentrations return to lower values. No or little decrease in concentration was observed for NTO and NQ immediately after flow interruption due to continued transformation in agreement with used k values (zero for both soils for NQ (Taylor et al., 2012) and 0.0009 and 0.0004 h^{-1} for NTO in Camp Swift and Camp Guernsey soils, respectively (Mark et al., 2016)).

For DNAN, no clear decrease in concentration was observed after flow interruption. However, concentrations of its transformation products, 2-ANAN and 4-ANAN, increased immediately after flow was resumed, indicating continued transformation and accumulation of transformation products throughout the columns. Absence of corresponding decreases in DNAN concentration is explained by a low transformation rate relative to error of the measurement. DNAN also did not experience increase in concentration following flow resumption like NTO and NQ due to its slower dissolution rate.

Transformation rate constants for DNAN were fixed in HYDRUS-1D simulations at the values determined in batch studies (Arthur et al., 2017), 0.0006 and 0.0033 h^{-1} for Camp Swift and Camp Guernsey, respectively. However, good agreement between simulated and measured BTCs for IF experiments that allow separating effects of dissolution and transformation on leachate concentrations, indicates that these values described observed patterns well.

Transformation rate constants previously obtained for NTO and DNA in column transport experiments are significantly higher than in batch experiments (Mark et al., 2016; Arthur et al., 2017; Mark et al., 2017) supposedly due to decrease in redox potential of the soil during saturated flow. However, current work indicates that batch transformation rate constants describe transport of dissolving explosives better. This phenomenon may be explained by DNAN toxicity to soil microorganisms (Dodard et al., 2013). High concentrations of DNAN during dissolution experiments may suppress microbial growth and cause decrease in transformation.

3.3. IMX-104

IMX-104 contains 53.0% NTO, 15.3% RDX, and 31.7% DNAN, 33.3% more NTO and 11.8% less DNAN than IMX-101. The behavior of NTO was similar to that of NTO in IMX-101, however it was retarded slightly more in both Camp Swift and Camp Guernsey soils. Similarly to patterns observed for IMX-101, NTO arrived before all other IM constituents in the IMX-104 and had the highest peak and steady-state concentrations (Fig. 4). NTO K_d's ranged from not significantly different from zero to 0.23 L·kg^{-1} (Table s3) which in some cases was higher than K_d values obtained for NTO in the IMX-101 dissolution studies and K_d values obtained in batch study experiments performed by Mark et al. (2016). RDX was the second IM compound to break through (Fig. 4). RDX exhibited retardation due to sorption, as demonstrated by the delay in RDX breakthrough relative to the conservative tracer. K_d values obtained for RDX ranged between 0.20 and 0.85 L·kg^{-1} with mean of 0.48 ± 0.14 L·kg^{-1} for Camp Swift and 0.37 ± 0.10 L·kg^{-1} for Camp Guernsey (Table s3). These values were on the lower end of the range of 0.12 to 8.2 L·kg^{-1} RDX K_d values reported by Brannon and Pennington (2002), as expected for soils with low OC content.

Concentrations of HMX in solution were smaller than those of RDX. HMX K_d's equaled 0.94 ± 0.17 L·kg^{-1} for Camp Swift and 0.72 ± 0.20 L·kg^{-1} for Camp Guernsey (Table s3), higher than RDX values and consistent with HMX K_d values reported by Brannon and Pennington (2002) (<1 L·kg^{-1}) and Dontsova et al. (2006) (0.22–0.36 L·kg^{-1}).

Breakthrough for DNAN, 2-ANAN, and 4-ANAN occurred at about 3 PVs (Fig. 4). All curves were asymmetrical. DNAN K_d values (0.66 ± 0.06 L·kg^{-1} for Camp Swift and 0.90 ± 0.26 L·kg^{-1} for Camp Guernsey) agreed very well with K_ds determined in in batch studies for the same soils (0.60 ± 0.20 L·kg^{-1} and 0.90 ± 0.10 L·kg^{-1}, respectively) and were similar to 1.2 ± 0.08 L·kg^{-1} determined in column studies for Camp Swift soil (Arthur et al., 2017). 2-ANAN K_d values were 1.20 ± 0.73 and 1.78 ± 1.13 L·kg^{-1} in Camp Swift and Camp Guernsey soils (Table s3).

Flow interruption during dissolution and transport of detonated IMX-104 had no effect on NTO in Camp Swift soil (Fig. 5). RDX concentrations, about 10 times HMX concentrations, first decreased and then increased after flow resumption, but predicted BTC showed smaller range of both decrease and increase, indicating that used RDX transformation rate constant (Brannon and Pennington, 2002), as well as dissolution rate calculated using it were lower than observed. Both RDX and HMX exhibited greater adsorption to the soil than NTO with RDX breakthrough occurring around 2 PVs and HMX at 4 PVs.

DNAN, 2-ANAN and 4-ANAN also adsorbed to the soil as indicated by the delay in the BTC (Fig. 5). Before flow interruption, DNAN and 2-ANAN concentrations decreased with time on the arrival wave. After resuming flow DNAN concentrations slightly decreased and 2-ANAN and 4-ANAN concentrations increased indicating continued DNAN transformation in Camp Swift soil, while concentrations of NTO, RDX, HMX,

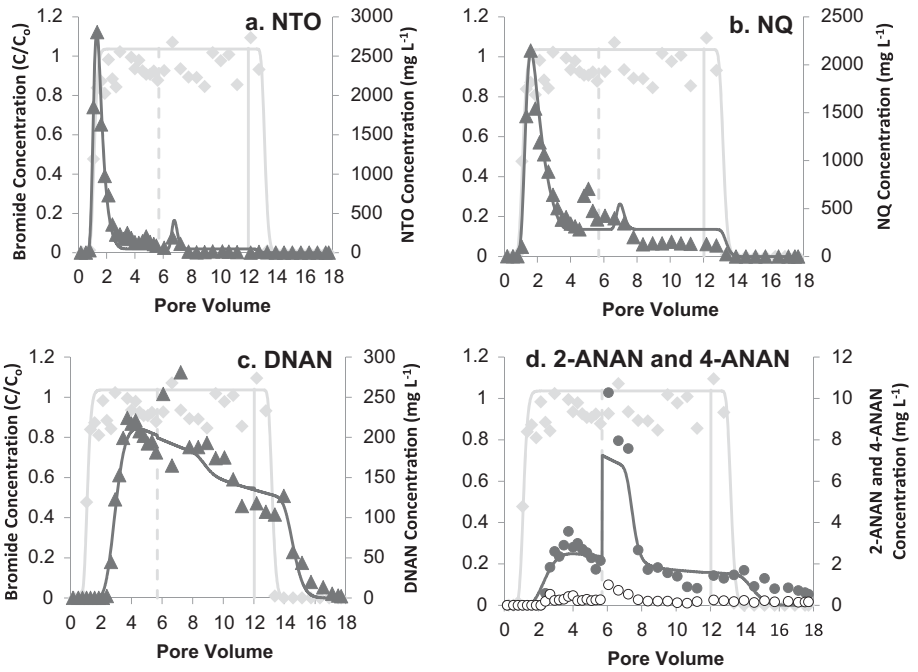

Fig. 3. Breakthrough curves for IM constituents dissolving from detonated IMX-101 in Camp Swift soil with flow interruption. Measured Br^- concentrations are presented in light grey diamonds, IM constituents, NTO, NQ, DNAN in dark grey triangles; and products of DNAN transformation, 2-ANAN and 4-ANAN, in solid and hollow circles, respectively. Lines present HYDRUS-1D simulation results. Vertical dashed line indicates start of 24-hr flow interruption and vertical grey solid grey line indicates switch to background solution.

DNAN and 2-ANAN all increased after flow interruption in Camp Guernsey soil (Figure S2). There were no significant differences in K_d values between undetonated and detonated IMX-104 nor were there differences in K_d values between the two soils used in the experiments.

A significant or highly significant correlation exists between HYDRUS-1D estimated values for Υ_{min} NTO and Υ_{min} RDX ($P = 0.0061$); Υ_{max} NTO and Υ_{max} DNAN ($P = 0.010$); and Υ_{min} HMX and Υ_{min} DNAN ($P = 0.018$) (Fig. 6). The Υ_{max} NTO and Υ_{max} DNAN correlation was also observed for the IMX-101 system. Some deviation from the predicted lines is expected for these correlations because of variability in composition of individual particles.

When comparing estimated dissolution parameters between treatments, we found that none of the parameters were significantly different between detonated and undetonated samples (Table 3, Table s3).

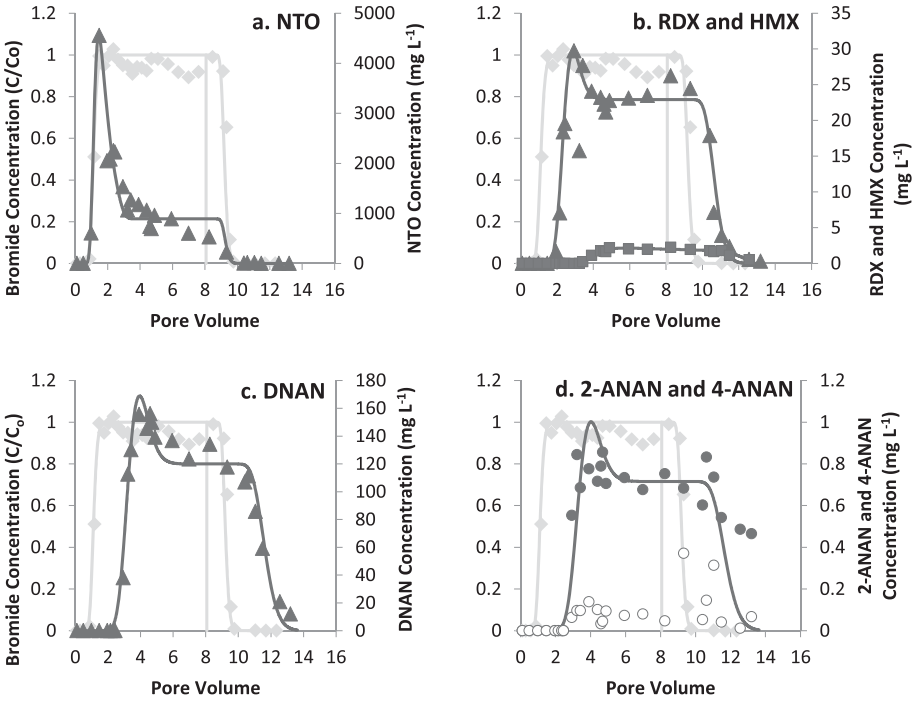

Fig. 4. Breakthrough curves for IM constituents from detonated IMX-104 particle in Camp Swift soil. Measured Br^- concentrations are presented in light grey diamonds, IM constituents, NTO, RDX, DNAN in dark grey triangles, HMX in dark grey squares; and products of DNAN transformation, 2-ANAN and 4-ANAN, in solid and hollow circles, respectively. Lines present HYDRUS-1D simulation results. Vertical grey solid line indicates switch to background solution.

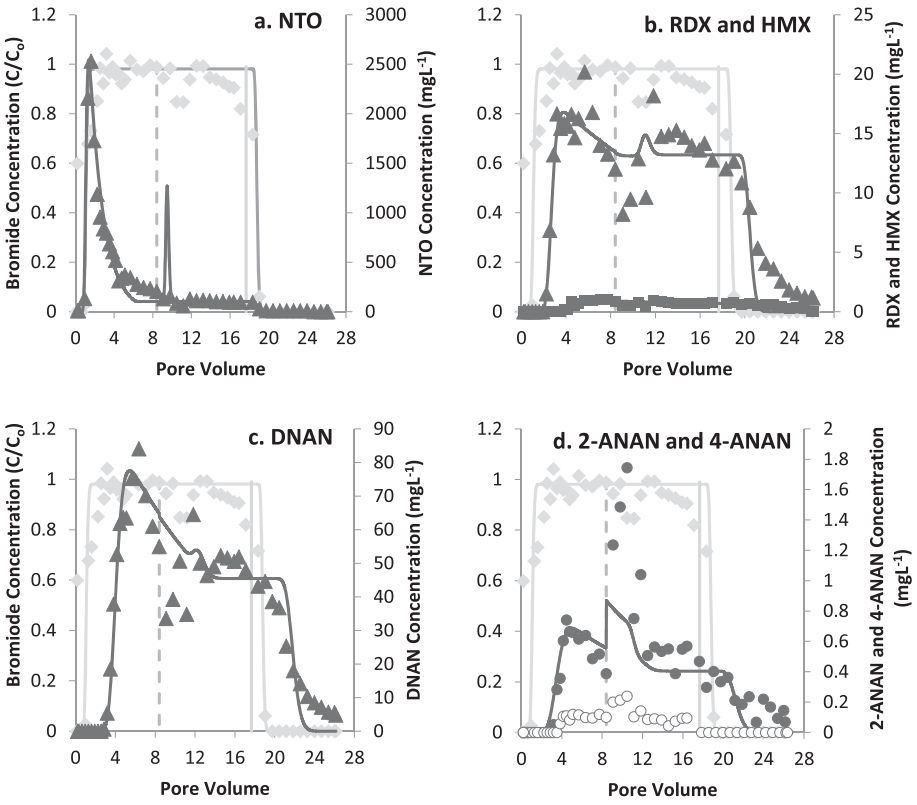

Fig. 5. Flow interruption breakthrough curves for IM constituents from detonated IMX-104 particle in Camp Swift soil. Measured Br^- concentrations are presented in light grey diamonds, IM constituents, NTO, RDX, DNAN in dark grey triangles, HMX in dark grey squares; and products of DNAN transformation, 2-ANAN and 4-ANAN, in solid and hollow circles, respectively. Lines present HYDRUS-1D simulation results. Vertical dashed grey line indicates start of 24-h flow interruption. Vertical solid grey line indicates switch to background solution.

Comparison of the dissolution parameters estimated here with the estimates obtained by Taylor et al. (2015b), same as for IMX-101 showed that their parameter estimates were lower than the estimates obtained from this study (Table s2) likely due to the size of the particle dissolved during analysis.

3.4. Comparison of IMX-101 and IMX-104

Dissolution rates are affected by the solubility of the compound, temperature, particle size and surface area, and agitation. During these experiments, constant temperature was maintained and the solid IMX particles were stationary on top of the soil profile, leaving the particle surface area (or exposed surface area of individual component of the formulations) and the solubility of the compounds (Table 1). Relative solubility of compounds manifest itself in higher estimated maximum and minimal dissolution rates for NTO compared to other IM constituents, while changing exposed surface area of individual IM components was responsible for observed patterns of dissolution.

IMX-101 and IMX-104 are made by melt-casting during which NTO, NQ, and RDX crystals are added to the molten DNAN. Since DNAN is less soluble than NTO and NQ, it can shield these compounds from dissolution after they are lost from the particle surface and thereby cause concentration decreases over time. Similarly, in IMX-104, RDX and DNAN remain after NTO is dissolved from the surface, constraining further dissolution of NTO. The shrinking core model is one way of conceptualizing dissolution behavior of the IMX particles: reactions occur first on the outer skin of the particle, then the zone of the reaction moves into the solid, leaving behind inert (in our case, less soluble) materials as well as exposing another layer of the reactant. As NTO is depleted from the outer surface of the particle, the dissolution front progresses deeper within the particle. This process continues and thus the unreacted core of the particle, where NTO remains, shrinks. Taylor et al. (2013) examined the physical changes undergone by insensitive munitions particles during dissolution. They confirmed that for IMX-101, NTO and NQ dissolved from the outside of the particles leaving behind thin bridges of DNAN, which dissolves more slowly. The resulting porous matrix allowed greater access of water to NTO and NQ in the particle interior, promoting their dissolution and subsequent advection with the moving water and diffusion to the particle exterior. While an analytical solution associated with the shrinking core model exists (e.g. Levenspiel, 1999, pages 569–570), an empirical equation (Eq. 1) was used to describe the observed patterns to simplify calculations.

IMX-101 and IMX-104 both contain NTO and DNAN in their formulations. IMX-104 contains 2.6 times more NTO than IMX-101 and 1.4 times less DNAN. The maximum and minimum dissolution rates are higher for NTO in IMX-101 than IMX-104 consistent with its larger percentage in the formulation. Though ratios between formulations for maximum and minimum dissolution rates were not the same (1.2 for Υ_{max} and 4.0 for Υ_{min}), they averaged to 2.6. When comparing the maximum and minimum dissolution for DNAN, we found that the dissolution rates of DNAN in IMX-104, were in fact higher than in 101, despite smaller DNAN percentage in the formulation (Tables 2, 3, s1, and s3). This could not be explained by differences in exposed surface area as we would expect that in IMX-101 fast dissolution of NTO and NQ will expose more of DNAN surfaces, while in IMX-104 less soluble RDX would persist and prevent further DNAN dissolution.

Dissolution model employed for HYDRUS-1D in these simulations, as previously used in Taylor et al. (2012), resulted in good fit to the initial parts of the BTC when concentrations rapidly increased and then decreased due to decrease in dissolution. In the later part of the BTC when model predicted no change in dissolution it worked better for RDX, HMX, DNAN, and NQ which had more constant dissolution, and less well for NTO which experienced continued slow decrease in concentrations (Figs. 1, 2, 4, 5). Mean R^2 value across all HYDRUS-1D simulations was 0.92 (Tables s1 and s3).

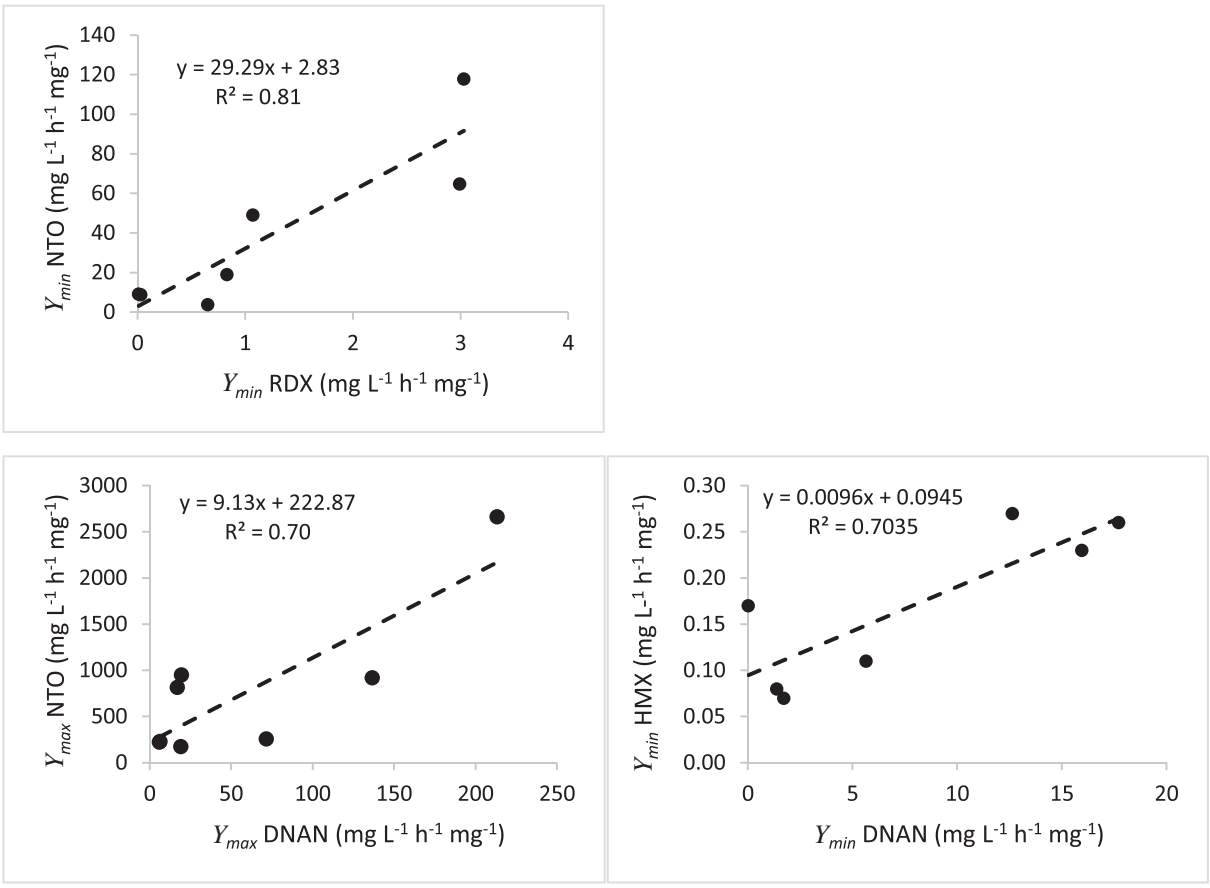

Fig. 6. Correlations between simulated initial and steady-state dissolution rates, Υ_{max} and Υ_{min}, of IM constituents, NTO, RDX, HMX, and DNAN, in IMX-104 formulation from continuous flow experiments.

Table 3
Mean dissolution parameters obtained by HYDRUS-1D for column saturated experiments involving IMX-104 in Camp Swift and Camp Guernsey soils. Decay constant, χ, and initial and steady-state dissolution rates, Υ_{max} and Υ_{min}, were estimated from explosives BTCs. FI = flow interruption, n = number of experiments included in the mean.

Treatment	χ	95% CI	Υ_{max}	95% CI	Υ_{min}	95% CI
			mg·L^{-1}·h^{-1}·mg^{-1}		mg·L^{-1}·h^{-1}·mg^{-1}	
NTO						
Detonated (n = 4)	0.07	0.08	996.42	1138.57	36.36	53.73
Undetonated (n = 4)	0.20	0.11	564.88	365.88	43.66	26.86
Detonated FI (n = 4)	0.16	0.04	725.34	252.10	20.41	14.62
Mean across IMX-104 (n = 12)	0.15	0.05	762.21	383.24	33.48	19.50
RDX						
Detonated (n = 4)	0.18	0.22	6.10	6.15	0.98	1.39
Undetonated (n = 4)	0.21	0.18	138.57	259.66	37.21	69.87
Detonated FI (n = 4)	0.16	0.16	4.35	2.85	2.33	1.48
Mean across IMX-104 (n = 12)	0.18	0.10	49.68	86.68	13.51	23.29
HMX						
Detonated (n = 4)	84.04	61.46	8.83	8.70	0.19	008
Undetonated (n = 4)	1.35	0.96	23.02	6.25	0.14	0.09
Detonated FI (n = 4)	0.05	0.07	0.31	0.20	0.18	0.06
Mean across IMX-104 (n = 12)	28.48	29.71	10.72	6.41	0.17	0.04
DNAN						
Detonated (n = 4)	0.28	0.23	93.70	96.95	8.77	9.17
Undetonated (n = 4)	0.24	0.43	28.53	28.63	5.97	4.64
Detonated FI (n = 4)	0.06	0.09	17.07	5.47	9.72	3.98
Mean across IMX-104 (n = 12)	0.19	0.16	48.43	36.46	8.15	3.45

3.5. pH of the IM solutions

The pH of effluent solutions of IMX-101 and IMX-104 was measured after the water interacted with the explosives and soil column. In solution, NTO is acidic as a result of the N—H bond dissociation and has a pKa of 3.67–3.76 (Lee et al., 1987; Smith and Cliff, 1999). Taylor et al. (2015a) showed that pH of NTO solutions is inversely related to their concentrations and can reach pH values as low as 2–3. During transport NTO solutions are buffered by reactions with the soil and the average pH of IMX-101 the outflow effluent solution was 8.44 ± 0.19 and the average pH of IMX-104 outflow effluent solution was 8.27 ± 0.26. However, for several PVs collected (Figure s3) when NTO concentrations were the highest, solutions also had lower pH values. pH of solutions entering soil matter both for fate of NTO itself, which can become deprotonated at higher pHs decreasing its adsorption to soils that possess net negative charge (Mark et al., 2016) and because of potential increase in mobility of metals in soils at low pHs.

3.6. Mass balance

IMX-101 (NTO, NQ, DNAN) and IMX-104 (NTO, RDX, DNAN) constituents were recovered in column effluent, soil extracts, and residual particle extracts. In addition to parent compounds, DNAN transformation products, 2-ANAN and 4-ANAN, were also recovered in both IMX-101 and 104 and HMX was recovered in IMX-104 studies. Mass balance calculations (Tables 4, s4) indicate that the majority of the individual compounds were recovered in effluent solution and in the residual particle. In IMX-101, NTO had the highest recoveries in solution followed by NQ, DNAN, 2-ANAN and 4-ANAN (Tables 4, s4). There were no significant

Table 4
Mass recoveries of IMX-101 and IMX-104 constituents in effluent, soil, and extractions of remaining IM particles relative to initial amount estimated based on defined composition during dissolution column transport studies. FI = flow interruption for 24 h, n = number of experiments included in the mean.

IMX-101	Solution recoveries				Soil recoveries						IMX particle recoveries		
Treatment	NTO	NQ	DNAN	2-ANAN	4-ANAN	NTO	NQ	DNAN	2-ANAN	4-ANAN	NTO	NQ	DNAN
	%	%	%	%	%	%	%	%	%	%	%	%	%
Detonated Mean (n = 4)	46.03	19.07	11.41	0.10	0.07	1.92	0.22	1.35	0.29	0.01	43.92	46.90	29.90
95% CI	32.96	17.33	14.02	0.05	0.07	2.09	0.02	0.46	0.11	0.00	30.94	29.67	17.60
Undetonated Mean (n = 4)	34.38	12.91	18.16	0.21	0.02	0.89	0.22	1.18	0.25	0.00	75.55	67.06	84.27
95% CI	21.54	8.53	28.99	0.20	0.01	0.08	0.03	0.24	0.11	0.00	10.25	8.15	43.44
Detonated FI Mean (n = 4)	73.43	80.51	32.13	2.52	0.25	0.07	0.08	0.37	0.02	0.01	5.25	10.82	52.89
95% CI	22.13	35.67	5.70	2.26	0.20	0.06	0.14	0.21	0.01	0.02	2.02	5.50	12.22
Mean across IMX-101 ($n = 12$)	51.28	37.50	20.57	0.95	0.11	0.96	0.17	0.97	0.18	0.01	41.36	41.11	58.03
95% CI	16.70	21.79	11.10	0.95	0.08	0.77	0.06	0.30	0.08	0.01	18.81	15.16	19.31

IMX-104	Solution recoveries						Soil recoveries						IMX particle recoveries			
Soils, treatment	NTO	DNAN	2-ANAN	4-ANAN	RDX	HMX	NTO	DNAN	2-ANAN	4-ANAN	RDX	HMX	NTO	DNAN	RDX	HMX
	%	%	%	%	%	mg	%	%	%	%	%	mg	%	%	%	mg
Detonated Mean (n = 4)	50.28	15.66	0.62	0.03	5.40	0.04	0.03	0.40	0.02	0.03	0.04	0.01	16.18	39.83	53.58	0.30
95% CI	8.34	8.67	0.91	0.01	2.75	0.02	0.00	0.12	0.01	0.03	0.01	0.01	13.34	4.70	25.37	0.12
Undetonated Mean (n = 4)	56.51	9.37	0.16	0.04	4.28	0.04	0.04	0.28	0.02	0.01	0.03	0.00	36.43	56.71	35.66	0.37
95% CI	9.66	6.10	0.05	0.02	2.74	0.02	0.01	0.08	0.00	0.01	0.00	0.00	4.11	23.35	48.03	0.34
Detonated FI Mean (n = 4)	79.07	26.50	0.53	0.12	11.74	0.07	0.12	0.45	0.01	0.04	0.28	0.01	7.07	45.05	45.36	0.27
95% CI	16.07	15.07	0.70	0.10	9.38	0.04	0.17	0.41	0.01	0.04	0.52	0.01	7.12	10.02	13.90	0.06
Mean across IMX-104 (n = 12)	67.74	18.88	0.48	0.07	7.89	0.06	0.07	0.41	0.02	0.03	0.14	0.00	20.15	49.01	67.81	39.43
95% CI	13.57	7.84	0.37	0.04	3.99	0.02	0.06	0.15	0.01	0.02	0.18	0.00	8.53	8.81	17.45	0.11

differences in solution recoveries of individual compounds in detonated versus undetonated IMX-101 but more NQ, DNAN, and 2-ANAN was removed in solution during flow interruption experiments for detonated samples due to their longer duration. For IMX-104, NTO had the highest recoveries in effluent followed by DNAN, RDX, 2-ANAN, 4-ANAN, and HMX (Tables 4, s4) and more NTO was recovered in solution for the interrupted flow experiments.

Recoveries in the soil were < 1% for all IM constituents. Low recoveries of the explosive compounds from the soil (Tables 4, s4) are related to experimental design: majority of munitions constituents should be desorbed from the soils and eluted by the time experiment was finished and soils extracted with acetonitrile. DNAN had the highest recoveries in soil for both IMX-101 and 104 consistent with the fact that its elution was not complete by the time experiment was ended due to its adsorption in the soil (Figs. 1, 2, 4, 5). It should be noted that while on the scale of individual munitions these compositions are well mixed, the particles are small and because of that can have somewhat varying composition amongst different particles. Hence, recoveries of each component in individual particles may exceed 100% of the calculated amount.

4. Conclusion

This study examined the dissolution, fate and transport behavior of IMX-101 and IMX-104, new IM formulations, in two soils. Insensitive munitions dissolution resulted in distinct elution patterns with high initial concentrations for highly soluble NTO and NQ quickly followed by lower and relatively constant concentrations in column effluent. Less soluble DNAN, RDX, and HMX had smaller or no initial peaks and effluent concentrations were lower and fairly steady over time. Flow interruption, as would be observed under natural rainfall conditions, resulted in increases in concentrations of energetics due to their continued dissolution from the particles. HYDRUS-1D software for modeling water flow and reactive transport of chemicals, modified to also simulate energetic compound dissolution from IM particles, successfully simulated dissolution and subsequent transport and transformation of these compounds, as well as the production and transport of their transformation products. Dissolution was represented by an initial (maximum) rate followed by exponential decrease to a constant (steady-state or minimum) rate. Estimated dissolution rates varied widely between the particles but were correlated between different components in the formulation.

NTO and NQ exhibited minimal retardation, while elution of DNAN, RDX, and HMX was delayed by adsorption to the soil. Estimated adsorption coefficients from HYDRUS-1D for each explosive compound were similar to those of pure NTO, NQ, DNAN, RDX, and HMX obtained from batch experiments, indicating that adsorption coefficients obtained from batch studies of pure explosives in solution can be used to reasonably represent transport of mixtures. DNAN transformed to 2-ANAN and 4-ANAN and under flow interruption conditions. NTO concentrations also decreased due to transformation. This indicates the potential for natural attenuation of IM constituents in soils through adsorption and transformation.

Acknowledgements

This work was funded by the Strategic Environmental Research and Development Program, SERDP, project ER-2220. We thank Dr. Andrea Leeson, SERDP Environmental Restoration Program Manager for her continued support. We are grateful to Anthony Di Stasio and Erika Rivera, US Army Armament Research, Development and Engineering Center (ARDEC), Picatinny Arsenal for providing IMX-101 and IMX-104; Bonnie M. Packer, Rosa Gwinn, Lisa DeGrazia, Bethany Keller, Jessica Milose, Amibeth Sheridan, Laurie Stenberg, Sarah Gettier, Army National Guard–Environmental Directorate and URS Corporation, Germantown, MD for collecting soils used in the experiments on Army National Guard installations.

Appendix A. Supplementary data

Supplementary data to this article can be found online at https://doi.org/10.1016/j.scitotenv.2017.11.307.

References

Arthur, J.D., Mark, N.W., Taylor, S., Šimunek, J., Brusseau, M.L., Dontsova, K.M., 2017. Batch soil adsorption and column transport studies of 2,4-dinitroanisole (DNAN) in soils. J. Contam. Hydrol. 199, 14–23.

Boddu, V.M., Abburi, K., Maloney, S.W., Damavarapu, R., 2008. Thermophysical properties of an insensitive munitions compound, 2,4-dinitroanisole. J. Chem. Eng. Data 53, 1120–1125.

Boyer, I., Miller, J.K., Watson, R.E., DeSesso II, J., Vogel, C.M., 2007. Comparison of the Relative Risks of CL-20 and RDX. Noblis Center for Science and Technology, Falls Church, Virginia.

Braida, W.J., Wazne, M., Ogundipe, A., Sen Tuna, G., Pavlov, J., Koutsospyros, A., 2012. Transport of nitrotriazolone (NTO) in soil lysimeters. Proceedings of Protection and Restoration of the Environment XI (Thessaloniki, Greece).
Brannon, J.M., Pennington, J.C., 2002. Environmental Fate and Transport Process Descriptors for Explosives. US Army Corps of Engineers. Engineer Research and Development Center, Vicksburg, MS.
Brusseau, M.L., 1994. Transport of reactive contaminants in heterogeneous porous media. Rev. Geophys. 32, 285–313.
Brusseau, M.L., Rao, P.S.C., Jessup, R.E., Davidson, J.M., 1989. Flow interruption: a method for investigating sorption nonequilibrium. J. Contam. Hydrol. 4, 223–240.
Brusseau, M.L., Hu, Q., Srivastava, R., 1997. Using flow interruption to identify factors causing nonideal contaminant transport. J. Contam. Hydrol. 24, 205–219.
Burrows, E.P., Rosenblatt, D.H., Mitchell, W.R., Parmer, D.L., 1989. Organic explosives and related compounds. Environmental and Health Considerations. Army Biomedical Research & Development Lab, Fort Detrick, MD.
Burton, D.T., Turley, S.D., Peters, G.T., 1993. Toxicity of Nitroguanidine, Nitroglycerin, Hexahydro-1,3,5-Trinitro-1,3,5-Triazine (RDX) and 2,4,6-Trinitrotoluene (TNT) to Selected Freshwater Aquatic Organisms: Final Report (Frederick, MD).
Chakka, S., Boddu, V.M., Maloney, S.W., Damavarapu, R., 2008. Prediction of Physicochemical Properties of Energetic Materials Via EPI Suite. American Institute of Chemical Engineers Annual Meeting, Philadelphia, PA.
Dave, G., Nilsson, E., Wernersson, A.S., 2000. Sediment and water phase toxicity and UV-activation of six chemicals used in military explosives. Aquat. Ecosyst. Health Manag. 3, 291–299.
Davies, P.J., Provatas, A., 2006. Characterisation of 2,4-Dinitroanisole: An Ingredient for Use in Low Sensitivity Melt Cast Formulations. Weapons Systems Division, Defence Science and Technology Organisation.
Deeter, D.P., 2000. Occupational Health (Textbook of Military Medicine — Part 3, Disease and the Environment). Dept. of the Army.
Dodard, S.G., Sarrazin, M., Hawari, J., Paquet, L., Ampleman, G., Thiboutot, S., Sunahara, G.I., 2013. Ecotoxicological assessment of a high energetic and insensitive munitions compound: 2,4-dinitroanisole (DNAN). J. Hazard. Mater. 262, 143–150.
Dontsova, K., Taylor, S., 2018. High Explosives: Their Dissolution and Fate in Soils. In: Shukla, M., Boddu, V., Steevens, J., Reddy, D., Leszczynski, J. (Eds.), Energetic Materials: From Cradle to Grave. Springer.
Dontsova, K.M., Yost, S.L., Simunek, J., Pennington, J.C., Williford, C.W., 2006. Dissolution and transport of TNT, RDX, and composition B in saturated soil columns. J. Environ. Qual. 35, 2043–2054.
Dontsova, K.M., Pennington, J.C., Yost, S., Hayes, C., 2007. Transport of nitroglycerin, nitroguanidine and diphenylamine in soils. Characterization and Fate of Gun and Rocket Propellant Residues on Testing and Training Ranges: Interim Report 1. Engineer Research and Development Center, Vicksburg, MS.
Dontsova, K.M., Chappell, M., Šimunek, J., Pennington, J.C., 2008. Dissolution and transport of nitroglycerin, nitroguanidine and ethyl centralite from M9 and M30 propellants in soils. Characterization and Fate of Gun and Rocket Propellant Residues on Testing and Training Ranges: Final Report. (ERDC TR-08-1). U.S. Army Engineer Research and Development Center, Vicksburg, MS.
Dontsova, K.M., Hayes, C., Šimunek, J., Pennington, J.C., Williford, C.W., 2009. Dissolution and transport of 2,4-DNT and 2,6-DNT from M1 propellant in soil. Chemosphere 77, 597–603.
Dontsova, K., Taylor, S., Pesce-Rodriguez, R., Brusseau, M., Arthur, J., Mark, N., Walsh, M., Lever, J., Šimůnek, J., 2014. Dissolution of NTO, DNAN, and Insensitive Munitions Formulations and Their Fates in Soils. Cold Regions Research and Engineering Laboratory, Hanover, NH (p. 92).
Etnier, E.L., 1986. Water Quality Criteria for Hexahydro-1,3,5-Trinitro-1,3,5-Triazine (RDX). Oak Ridge National Laboratory, Oak Ridge, TN.
Glover, D., Hoffsommer, J., 1973. Thin-layer chromatographic analysis of HMX in water. Bull. Environ. Contam. Toxicol. 10, 302–304.
Haag, W.R., Spanggord, R., Mill, T., Podoll, R.T., Chou, T.-W., Tse, D.S., Harper, J.C., 1990. Aquatic environmental fate of nitroguanidine. Environ. Toxicol. Chem. 9, 1359–1367.
Haderlein, S.B., Weissmahr, K.W., Schwarzenbach, R.P., 1996. Specific adsorption of nitroaromatic explosives and pesticides to clay minerals. Environ. Sci. Technol. 30, 612–622.
Hawari, J., Perreault, N., Halasz, A., Paquet, L., Radovic, Z., Manno, D., Sunahara, G.I., Dodard, S., Sarrazin, M., Thiboutot, S., Ampleman, G., Brochu, S., Diaz, E., Gagnon, A., Marois, A., 2012. Environmental Fate and Ecological Impact of NTO, DNAN, NQ, FOX-7, and FOX-12 Considered as Substitutes in the Formulations of Less Sensitive Composite Explosives. National Research Council Canada.
Hawari, J., Monteil-Rivera, F., Perreault, N.N., Halasz, A., Paquet, L., Radovic-Hrapovic, Z., Deschamps, S., Thiboutot, S., Ampleman, G., 2015. Environmental fate of 2,4-dinitroanisole (DNAN) and its reduced products. Chemosphere 119, 16–23.
Jenkins, T.F., Pennington, J.C., Ranney, T.A., Berry Jr., T.E., Miyares, P.H., Walsh, M.E., Hewitt, A.D., Perron, N.M., Parker, L.V., Hayes, C.A., Wahlgren, E.G., 2001. Characterization of Explosives Contamination at Military Firing Ranges. Engineer Research and Development Center.
Le Campion, L., Giannotti, C., Ouazzani, J., 1999. Photocatalytic degradation of 5-nitro-1,2,4-triazol-3-one NTO in aqueous suspension of TiO_2. Comparison with Fenton oxidation. Chemosphere 38, 1561–1570.
Lee, K.-Y., Chapman, L.B., Cobura, M.D., 1987. 3-Nitro-1,2,4-triazol-5-one, a less sensitive explosive. Journal of Energetic Materials 5, 27–33.
Levenspiel, O., 1999. Chemical Reaction Engineering. 3rd ed. John Wiley & Sons, New York.
London, J.O., Smith, D.M., 1985. A Toxicological Study of NTO. Los Alamos National Laboratory Report.
Mark, N., Arthur, J., Dontsova, K., Brusseau, M., Taylor, S., 2016. Adsorption and attenuation behavior of 3-nitro-1,2,4-triazol-5-one (NTO) in eleven soils. Chemosphere 144, 1249–1255.
Mark, N., Arthur, J., Dontsova, K., Brusseau, M., Taylor, S., Šimůnek, J., 2017. Column transport studies of 3-nitro-1,2,4-triazol-5-one (NTO) in soils. Chemosphere 171, 427–434.
Mirecki, J.E., Porter, B., Weiss, C.A., 2006. Environmental Transport and Fate Process Descriptors for Propellant Compounds. U.S. Army Engineer Research and Development Center, Vicksburg, MS.
Olivares, C., Liang, J., Abrell, L., Sierra-Alvarez, R., Field, J.A., 2013. Pathways of reductive 2,4-dinitroanisole (DNAN) biotransformation in sludge. Biotechnol. Bioeng. 110, 1595–1604.
Pennington, J.C., Jenkins, T.F., Ampleman, G., Thiboutot, S., 2004. Distribution and Fate of Energetics on DoD Test and Training Ranges: Interim Report 4. U.S. Army Engineer Research and Development Center, Vicksburg, MS.
Richard, T., Weidhaas, J., 2014. Dissolution, sorption, and phytoremediation of IMX-101 explosive formulation constituents: 2,4-dinitroanisole (DNAN), 3-nitro-1,2,4-triazol-5-one (NTO), and nitroguanidine. J. Hazard. Mater. 280, 561–569.
Šimůnek, J., van Genuchten, M.T., 2008. Modeling nonequilibrium flow and transport with HYDRUS. Vadose Zone J. 7 (Special Issue "Vadose Zone Modeling"), 782–797.
Šimůnek, J., Šejna, M., Saito, H., Sakai, M., van Genuchten, M.T., 2008. The HYDRUS-1D Software Package for Simulating the Movement of Water, Heat, and Multiple Solutes in Variably Saturated Media, Version 4.0. HYDRUS Software Series 3. Department of Environmental Sciences, University of California Riverside, Riverside, California, USA (p. 315).
Singh, J., Comfort, S.D., Hundal, L.S., Shea, P.J., 1998. Long-term RDX sorption and fate in soil. J. Environ. Qual. 27, 572–577.
Smith, M.W., Cliff, M.D., 1999. NTO Based Explosive Formulations: A Technology Review. Weapons Systems Division, Aeronautical and Maritime Research Laboratory.
Sokkalingam, N., Potoff, J.J., Boddu, V.M., Maloney, S.W., 2008. Prediction of environmental impact of high-energy materials with atomistic computer simulations. ADM002187. Proceedings of the Army Science Conference (26th) Held in Orlando, Florida on 1–4 December 2008.
Spear, R.J., Louey, C.N., Wolfson, M.G., 1989. A Preliminary Assessment of 3-Nitro-1,2,4-Triazol-5-One (NTO) as an Insensitive High Explosive. DSTO Materials Research Laboratory, Maribyrnong, Australia (p. 38).
Sunahara, G.I., 2009. Ecotoxicology of Explosives. CRC Press, Boca Raton.
Taylor, S., Lever, J.H., Fadden, J., Perron, N., Packer, B., 2009. Simulated rainfall-driven dissolution of TNT, Tritonal, Comp B and Octol particles. Chemosphere 75, 1074–1081.
Taylor, S., Richardson, C., Lever, J.H., Pitt, J.S., Bigl, S., Perron, N., Bradley, J.P., 2011. Dissolution of nitroglycerin from small arms propellants and their residues. International Journal of Energetic Materials and Chemical Propulsion 10, 397–419.
Taylor, S., Dontsova, K., Bigl, S., Richardson, C., Lever, J., Pitt, J., Bradley, J.P., Walsh, M., Šimůnek, J., 2012. Dissolution Rate of Propellant Energetics from Nitrocellulose Matrices. Cold Regions Research and Engineering Laboratory, Hanover, NH.
Taylor, S., Ringelberg, D.B., Dontsova, K., Daghlian, C.P., Walsh, M.E., Walsh, M.R., 2013. Insights into the dissolution and the three-dimensional structure of insensitive munitions formulations. Chemosphere 93, 1782–1788.
Taylor, S., Dontsova, K., Walsh, M.E., Walsh, M.R., 2015a. Outdoor dissolution of detonation residues of three insensitive munitions (IM) formulations. Chemosphere 134, 250–256.
Taylor, S., Park, E., Bullion, K., Dontsova, K., 2015b. Dissolution of three insensitive munitions formulations. Chemosphere 119, 342–348.
U. S. Environmental Protection Agency, 1994. SW846 Method 8330. Nitroaromatics and Nitramines by HPLC. Office of Solid Waste and Emergency Response, Washington, DC.
Walsh, M.R., Walsh, M.E., Ramsey, C.A., Brochu, S., Thiboutot, S., Ampleman, G., 2013. Perchlorate contamination from the detonation of insensitive high-explosive rounds. J. Hazard. Mater. 262, 228–233.
Walsh, M.R., Walsh, M.E., Ramsey, C.A., Thiboutot, S., Ampleman, G., Diaz, E., Zufelt, J.E., 2014. Energetic residues from the detonation of IMX-104 insensitive munitions. Propellants, Explosives, Pyrotechnics 39, 243–250.
Yoon, J.M., Oh, B.T., Just, C.L., Schnoor, J.L., 2002. Uptake and leaching of octahydro-1,3,5,7-tetranitro-1,3,5,7-tetrazocine by hybrid poplar trees. Environ. Sci. Technol. 36, 4649–4655.